Hindawi
International Transactions on Electrical Energy Systems
Volume 2022, Article ID 2669061, 12 pages
https://doi.org/10.1155/2022/2669061

Research Article

Reliability Evaluation of Nondispatchable Energy Sources in Generation Planning: A Wind Electrical System Case Study

Anant Milan Khalkho and Dusmanta Kumar Mohanta

Birla Institute of Technology, Mesra, Ranchi 834008, India

Correspondence should be addressed to Dusmanta Kumar Mohanta; dkmohanta@bitmesra.ac.in

Received 27 December 2021; Revised 23 March 2022; Accepted 21 April 2022; Published 24 June 2022

Academic Editor: Sujin Bureerat

Summary. Generation planning is an important aspect of the probabilistic production simulation (PPS) process for power systems. The inclusion of nondispatchable energy sources in the conventional system needs efficient algorithms for reliability evaluation. Moreover, it is crucial to represent the availability of nondispatchable energy sources with a suitable probability distribution function (PDF) that can be easily integrated with the conventional system. The present work extends the generation reliability to include nondispatchable energy sources in the reliability evaluation methodology. The wind electrical system (WS) is represented using a simple wind speed model based on the normal distribution function. The multistate wind speed model based on the mean and standard deviation of wind speed at a particular site is integrated with the conventional system for reliability study. The proposed fast Fourier transform (FFT)-based method eliminates extensive calculations encountered in the conventional approach due to cumbersome time-domain convolution. The efficacy of the methodology is validated with the case studies using the IEEE RTS-wind system with loss of load probability (LOLP) and expected energy not served (EENS) reliability indices.

1. Introduction

One of the goals of generation planning is to ensure a reliable power supply to the consumers. Recently, the global climatic concerns have given impetus to incorporate more renewable energy sources. Renewable energy sources are intermittent in nature. Particularly, wind energy generation is quite variable in nature due to its dependence on factors such as wind speed, and density of air. Such variable energy resources thus come under a category of nondispatchable energy sources [1, 2], and incorporation of these sources in generation planning is quite complex [3]. Wind energy has a significant share in nondispatchable energy generation due to its expansion in recent years [4, 5]. Therefore, generation planning should incorporate the stochastic behavior of wind along with the generator outages. Furthermore, the conventional dispatchable units (DUs) are represented by a model representing two states, but due to large variations, wind speed-based nondispatchable units (NDUs) require a multistate representation, which is complex. The uncertainties in nondispatchable generation can be modeled using PDF [6], which can be correlated with the generated power and integrated with PPS to determine the generation adequacy and reliability of the system.

1.1. Motivation. For efficient generation planning, it is also necessary to model the uncertainties associated with the DUs, which can be done by representing them in terms of their probabilities [7]. The most significant uncertainty in generation planning is the forced outage of generators [8].

The interaction of load probabilities, with the uncertainties associated with all the connected generating units, forms the basis for the probabilistic load model (PLM) used for reliability analysis [9]. PLM is a continuous modification of the load duration curve (LDC) considering generational uncertainties. LDC determines the time duration of load demands arranged in descending order in a given time interval [10], which can also be represented by the probability of occurrence of a particular demand in a given time

interval. In order to obtain PLM, the probabilistic model of each generator is convolved multiple times with the LDC. With the increase in generating units, the convolution process becomes cumbersome and time-consuming. The complexity and memory requirement for convolution further increases with the involvement of multistate renewable generation sources. With ever-increasing demand and generation requirements, an efficient algorithm with minimal computation time is required. The multiple steps required for convolution operation, performed in the time-domain conventionally, can be reduced to a single step with the application of the fast Fourier transform (FFT) algorithm [11]. This requires efficient probabilistic modeling of the generation sources to obtain the reliability indices.

The motivation of the present work is to integrate the uncertainty associated with wind farms with the probabilistic generation of the DUs and reduce the computational time and complexity of generation planning.

1.2. Related Literature. In recent years, numerous multistate models for wind turbines and reliability assessments of wind integrated power systems have been suggested due to the integration of wind energy systems (WS) into the conventional power system. The proposed works have concentrated on the reliability of protection systems [12], reliability considering elements connected to the power system network [13, 14], reliability enhancement using control strategies [15, 16], and reliability considering reactive power optimization [17]. However, the basic requirement of a power system is to satisfy the load demands considering the existing and upcoming system facilities [18], which needs to be dealt with on a priority basis. Although significant work has been done related to adequacy of generation considering conventional generators, adequacy studies considering wind integrated power system demands attention [19]. The amount of energy generated by wind farms varies with wind speed, depending on the farms' location. Hence, wind farms need to be represented by a common multistate wind speed model [20], representing uncertainty in wind generation. Also, the number of iterations for PLM computation increases with the increase of states, which needs to be simplified.

Reliability assessment of wind farms considering wind intermittency and parameters related to wind turbines have been reported in [21, 22]. The methods consider wind-related uncertainties, but the conventional generators have not been taken into account. Although combined reliability evaluation considering wind farms and conventional generators have been reported in [23], the methods do not consider common wind speed model considering wind farms at different locations. References [24, 25] have taken into account wind models that consider topological variations, but the reliability evaluation methodologies of wind energy-based power systems are complex. The reliability assessment of power systems with multistate energy sources requires complicated and time-consuming calculations. Therefore, it is imperative to use digital signal processing (DSP) tools, which can reduce the computational burden. A frequency-domain approach to calculate the reliability of the system considering solar irradiation intermittency has been proposed in [26]; however, the method has not been implemented for wind speed intermittency.

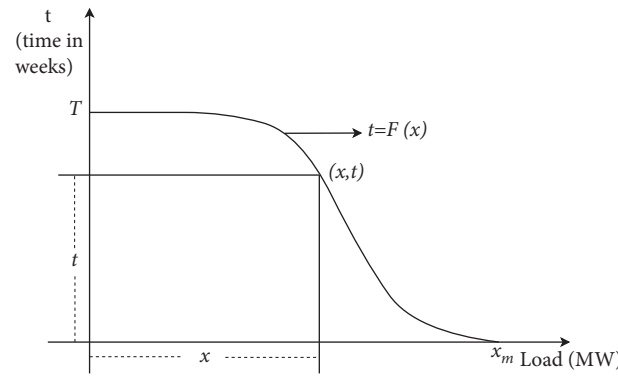

Figure 1: Representation of load duration curve.

1.3. Innovative Contributions. The power generation capacity of nondispatchable energy sources is dependent on nongovernable factors. The factors can be accounted for in reliability studies if they are represented by their occurrence probability. Wind speed, which is a nongovernable factor of WS, depends on the geographical conditions of the site, which can be represented by a PDF divided into multiple states. The reliability evaluation involves the interaction of this multistate model, the load behavior, and the other generation uncertainties. Hence, a simple algorithm is required to represent the interactions to minimize the time and memory requirements of the processor. The following are the innovative contributions of the current work in comparison to the existing literature:

(i) Impact assessment of grid-integrated nondispatchable energy sources having variable generation on reliability in combination with PLM

(ii) Extension of generation reliability evaluation to incorporate nondispatchable energy sources using multistate generation model

(iii) Frequency-domain approach for simplification of the process involved in the convolution of probabilistic multistate generation model with probabilistic load model

2. Reliability Modeling of Generating Sources

2.1. Reliability Model for Dispatchable Unit. Generation planning is an essential part of power system probabilistic simulation. In order to achieve an appropriate planning scheme, the simulation has to be run multiple times, and hence, efficient functions are required to represent the generation-load uncertainty. This can be done through PLM, which is derived from transformed LDC (where the axes are interchanged to represent the time duration as a function of the load) that expresses the duration of varying loads, as shown in Figure 1. In the figure, T is the duration of time for

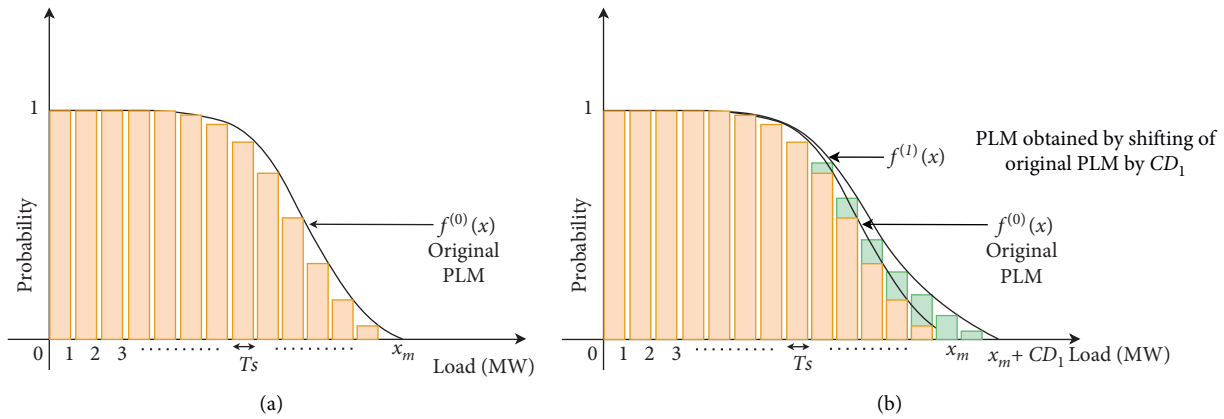

Figure 2: (a) The PLM based on transformed LDC and (b) the modified PLM considering outage of single generator.

the investigation, and x_m is the maximum connected load in the system (in MW). Also, (x,t) is the point on the curve, representing the time duration t for which load exceeds the value x and is expressed as $t = F(x)$. PLM is a representation of load (in MW) with associated probability sampled with a load interval of T_s MW as shown in Figure 2(a). The probability "p" that the load is $\leq x$ can be calculated from (1), which is used to obtain PLM from transformed LDC. To understand this consider a system having a base load of 1,800 MW operating for 52 weeks(T), a load of 1,881 MW operating for 44 weeks, a load of 2,280 MW operating for 31 weeks, and a load of 2,850 MW operating for 1 week. The corresponding probabilities of loads $\leq$ given values used to obtain PLM are $(52/52 = 1)$, $(44/52 = 0.84)$, $(31/52 = 0.59)$, and $(1/52 = 0.01)$, respectively. The total energy (E_L) under the transformed LDC is given by (2), which is equal to the energy under PLM.

$$\text{pr} = f(x) = \frac{F(x)}{T}, \tag{1}$$

$$E_L = \int_0^{x_m} F(x)\mathrm{d}x. \tag{2}$$

The forced outage of DUs has a tremendous impact on the available power, which may occur due to aging of units, failure of turbine and boiler, noncompliance with the safety norms, and so on [27, 28]. Considering the outage of DU as an individual event, the probability of outage of each unit can be modeled into two states. The probability of the failure state is given as forced outage rate (FOR) "q" and the probability of normal state is represented as $p = (1 - q)$." The PLM can be constructed using FOR, based on recursively adding one unit at a time by convolution process. The formulation of PLM can be represented in pictorial form, as shown in Figure 2.

The original load duration curve can be represented as the original PLM $f^{(0)}(x)$ given in Figure 2, illustrating the load delivered by all generating units with associated probabilities. The PLM is sampled, with each sample having an interval T_s. The curve is modified in accordance with the priority of the operation of DUs. The outage of dispatchable unit DU_1 with a capacity of CD_1 is represented by the shifting of the original curve by CD_1 as shown in Figure 2, mathematically represented as a convolution of original load duration curve and probability distribution of dispatchable unit DU_1 given by (3) [29]. The generalized equation to calculate the PLM for the outage of the unit DU_α is given by (4).

$$f^{(1)}(x) = f^{(0)}(x) \otimes \text{DU}_1 = p_1 f^{(0)}(x) + q_1 f^{(0)}(x - \text{CD}_1), \tag{3}$$

$$f^{(\alpha)}(x) = f^{(\alpha-1)}(x) \otimes \text{DU}_\alpha = p_\alpha f^{(\alpha-1)}(x) + q_\alpha f^{(\alpha)}(x - \text{CD}_\alpha). \tag{4}$$

The PLM represents the outage of the dispatchable unit by an increase in load demand, which further signifies the increase in energy as shown by the colored region in Figure 2. If the system has "g" dispatchable units with a total capacity CD_g, the PLM has a maximum capacity $x_m + \text{CD}_g$.

2.2. Modeling of Nondispatchable Units for Reliability Analysis. The DU outage is represented by a two-state model; however, NDUs have uncertainties having multiple states. Therefore, to include uncertainties with the units for reliability evaluation, multistate models representing them should be taken into account. If the uncertainty related to a DU has N_γ states, then the probability of generating $\text{NDC}_i\,(i = 0, 1, 2, \ldots, N_\gamma - 1)$ power states are $\text{pr}_{\text{NDC}i}\,(i = 0, 1, 2, \ldots, N_\gamma - 1)$ and is shown in Figure 3.

$$\text{NDC}_i + \overline{\text{NDC}_i} = \text{NDC}_\beta, \tag{5}$$

where NDC_β represents the maximum capacity of the wind farm. All wind farms' power states must fulfill the probability constraint given by

$$\sum_{i=0}^{N_\gamma - 1} \text{pr}_{\text{NDC}i} = 1. \tag{6}$$

The convolution formula to obtain PLM after integrating WS to represent the variability of power can be obtained by the modification of the formula obtained for dual state generating units. If the outage of (α) dispatchable units has been taken into account for generation planning and the

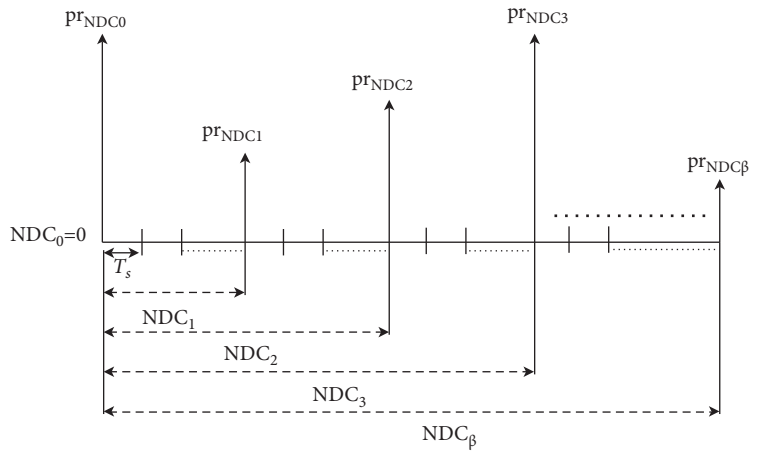

Figure 3: Power states of nondispatchable units with probabilities.

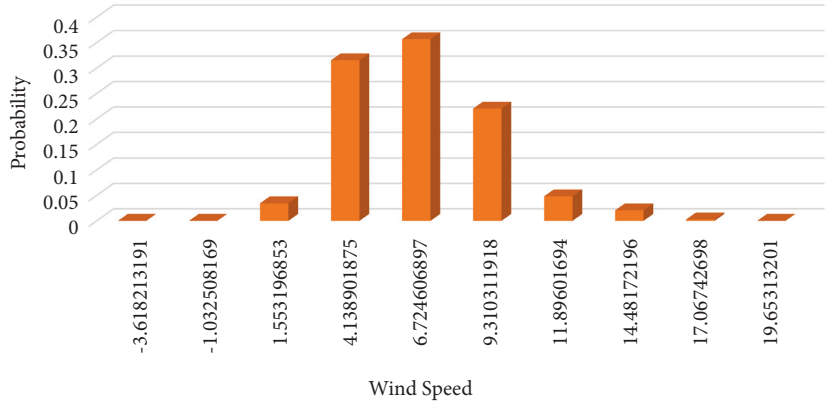

Figure 4: A 10-step model for the San Francisco Bay Area.

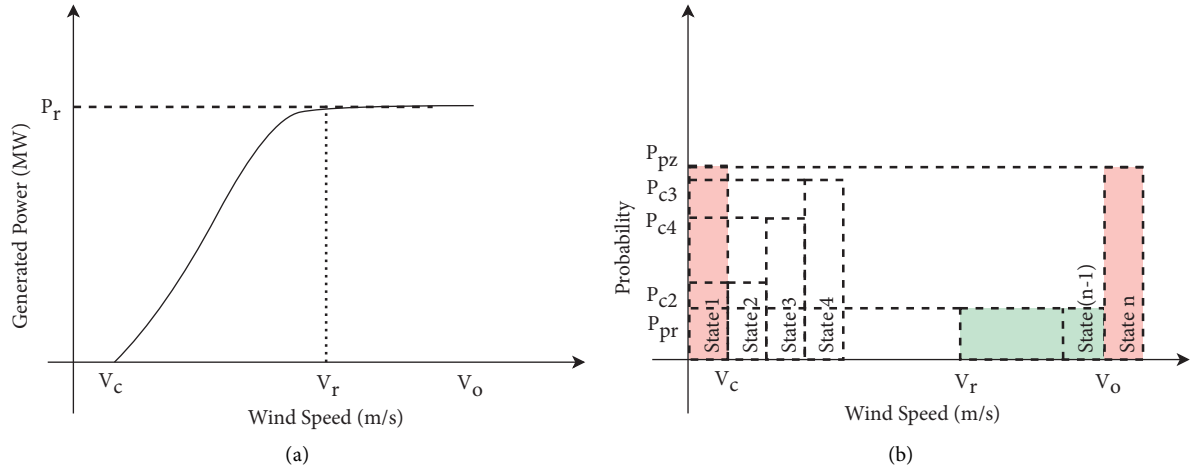

Figure 5: (a) The speed power curve of wind turbine and (b) multistate probability representation of power with respect to wind speed.

convolution of PLM, $f(x)$ is performed. For the addition of a multistate nondispatchable generating unit ND_j, having power state NDC_i with a probability pr_{NDCi}, the equivalent load shared by generating unit is $(x + NDC_i)$. This is mathematically represented by shifting of PLM to the right by $N\ DC_i$, and hence, the curve is modified to $f(x - NDC_i)$ having a probabilitypr_{NDCi}. Hence, the final PLM is a weighted sum of all the generating states, given by

$$f^{(j)}(x) = \sum_{i=1}^{N_\gamma} \left[pr_{NDCi} f^{(j-1)}(x - NDC_i) \right]. \quad (7)$$

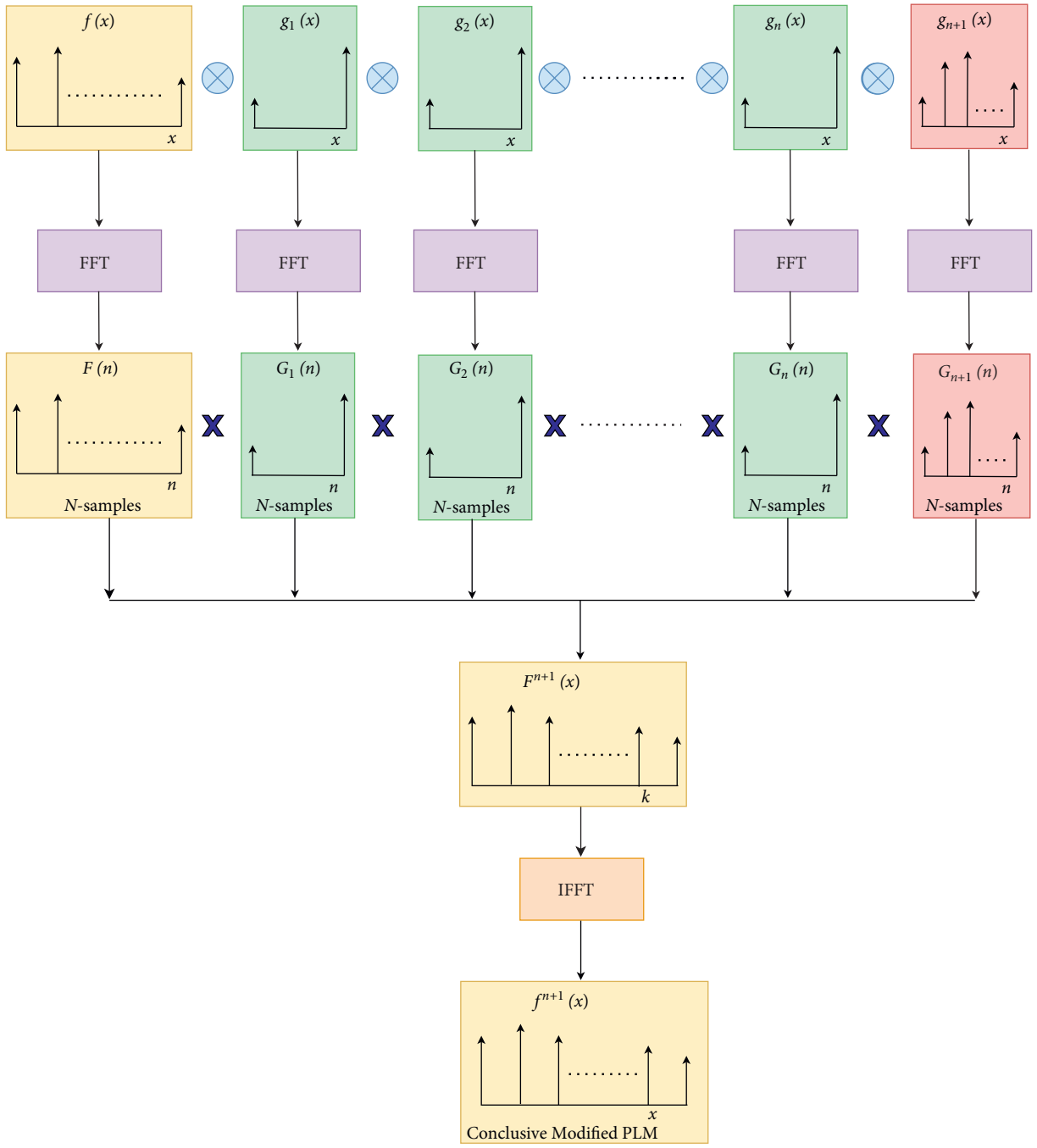

Figure 6: Representation of FFT algorithm for calculation of PLM.

When $N_\gamma = 1$, equation (7) reduces to (4), and when $j = 1$, $f^{(j-1)}$ is taken as $f^{(\alpha)}$.

3. Wind Speed Uncertainty Model

Several methodologies for calculating wind farm output power have been proposed [30, 31]. The reliability analysis of a wind energy-based system requires a simplistic wind speed model that is easy to integrate with the conventional generating system. The output of the wind farms is wind speed dependent, which is variable in nature. This section elaborates on the wind speed model described in [20], taking into account the mean of wind speed (μ) and the standard deviation (σ) of past available wind data. The correlation between the varying wind speed and forced outage of generating units is also discussed.

3.1. Wind Speed Model for Multiple Sites. Wind speeds obtained from various locations very closely fit the Weibull PDF. The shaping parameters of the distribution vary with different location and are difficult to calculate. However, the probability distribution of wind speeds can be approximated to normal distribution [20] by calculating the mean and

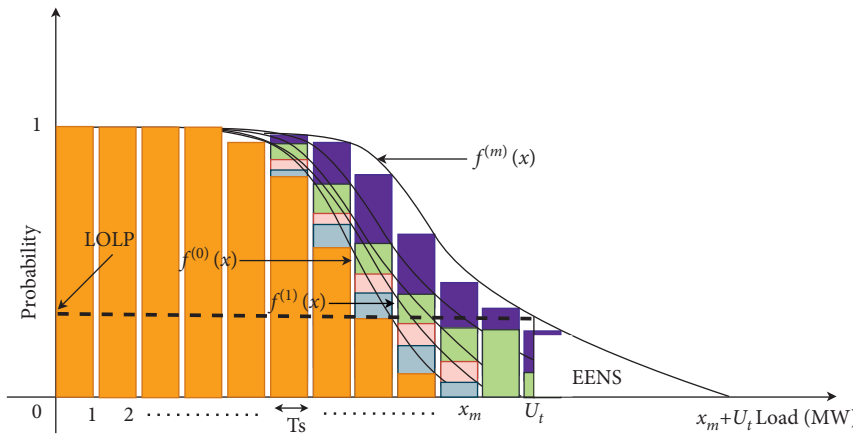

Figure 7: PLM for multiple generating units.

standard deviation of past wind speed data. To consider wind speeds during extreme weather conditions, the distribution is taken up to 10σ. For reliability evaluation purposes, the PDF is divided into N_{st} number of states and the width of each state being $(10\sigma/N_{st})$. If $\mathrm{MP}_{sti}\,(i = 0, 2, \ldots, N_{st} - 1)$ is the midpoint of the states, then the midpoint of each state can be calculated from (8), and the probability of each step is obtained from (9).

$$\left.\begin{aligned}\mathrm{MP}_{sti} &= \mu + \left(10\sigma/N_{st}\right) \times \left(i - 0.5 \times N_{st}\right) \quad \text{if } N_{st} \text{ is even}\\ &= \mu + \left(10\sigma/N_{st}\right) \times \left(i - 0.5 \times \left(N_{st} + 1\right)\right) \quad \text{if } N_{st} \text{ is odd}\end{aligned}\right\}, \tag{8}$$

$$p_{sti} = \frac{N_{spi}}{\left(8760 \times N_y\right)}, \tag{9}$$

where N_{spi} represents the total wind speed data points for a particular state and N_y is the wind speed data points obtained in a year. If multiple sites for wind farms are taken into account, the probabilities of individual sites can be combined to obtain a common wind speed probability for multiple locations. The common wind speed probability $P_{sti}\,(i = 0, 1, 2, \ldots, N_{st} - 1)$ of individual states for different sites represented by "j" is obtained by taking the average of probabilities $P_{stij}\,(j = 1, 2, \ldots, N_s)$ for N_s sites into consideration. A 10-step model is used for the present work based on [20] to represent the multistate wind as shown in Figure 4 for the San Francisco Bay Area, with the probability and midpoint of each state indicated. The negative value of wind speed is ignored as it has no significance. The wind speeds are obtained from [32], and each wind site indicates an individual farm.

3.2. Common Wind Power Generation Model. The power generated by a particular wind speed at different sites can be obtained from the speed-power curve of the wind turbine generator. The wind turbine generator starts generating power at wind speed V_c, and the generator is shut off after wind speed V_o for safety reasons. Rated power P_r is achieved between rated speed V_r and V_o the power curve for the wind generator, and multistate probability representation of power with respect to wind speed is shown in Figure 5. The power-speed relation between speeds V_c and V_r is nonlinear, and the generated power by a wind turbine $\mathrm{PW}_i\,(i = 0, 1, 2, \ldots, N_{st} - 1)$ for a given speed state $\mathrm{MP}_{sti}\,(i = 0, 1, 2, \ldots, N_{st} - 1)$ is given by

$$\begin{aligned}\mathrm{PW}_i &= 0, 0 \le \mathrm{MP}_{sti} < V_c,\\ &= P_r\left(A + B \times \mathrm{MP}_{sti} + C \times \mathrm{MP}_{sti}^2\right), \quad V_c \le \mathrm{MP}_{sti} < V_r,\\ &= P_r, \quad V_r \le \mathrm{MP}_{sti} < V_o,\\ &= 0, \quad V_o < \mathrm{MP}_{sti}.\end{aligned} \tag{10}$$

The constants A, B, and C have been calculated from [21].

The output of the wind turbine generator is zero when the wind speed is less than V_c and P_r when the wind speed is greater than V_o. Wind speed states corresponding to these values can therefore be combined into a single combined state whose probability P_{pz} is given by (11). The output power is rated power for wind speeds between V_r and V_o. These states can also be combined into a single state, and the probability of the combined state P_{pr} is given by (12).

$$P_{pz} = \sum P_{sti} \quad \text{for } 0 \le \mathrm{MP}_{sti} < V_c \text{ or } V_o < \mathrm{MP}_{sti}, \tag{11}$$

$$P_{\mathrm{pr}} = \sum P_{sti} \quad \text{for } V_r \le \mathrm{MP}_{sti} \le V_o. \tag{12}$$

4. Reliability Evaluation Methodology Using FFT

4.1. FFT for PLM. The convolution process to obtain PLM is given by (4) and (7), which becomes tedious to perform when generating units increase due to a large number of convolutions involved. Also, the number of data points obtained after each convolution increases twofold, which increases the memory requirement. FFT converts the sampled-time domain signal to the frequency domain, and thus, the time-domain convolution process is transformed to term-by-term multiplication. If $f[x]$ and $g[x]$ are two discrete time-domain signals, the signals are converted to $F(n)$ and $G(n)$ after FFT and are shown in the following equation [11]:

$$f[x] \otimes g[x] \overset{\text{FFT}}{\underset{\text{IFFT}}{\rightleftharpoons}} F(k) * G(k). \tag{13}$$

The FFT algorithm minimizes the number of computations required for discrete Fourier transform (DFT) calculations. The number of data points used for computation of FFT algorithm should satisfy (14), where S is an integer. A signal $f(x)$ can be represented by r impulse function with a scaling factor a_m, shifted by b_m and given by (15). This equation can be represented by a uniform shifting of pulses, with each pulse having a size Δx given by (16). The signal obtained is transformed to the frequency domain using (17), where $n = 0,1,2, \ldots, N-1$; $k = 0, 1, 2, \ldots, N-1$; and $W = e^{j2\pi/N}$. The signal after convolving in the frequency domain needs to be converted back to the time domain and is given by (18). The sampling points for the present work are calculated based on (19) [33], where $T_0 = x_m + U_t$ as the present work performs reliability evaluation based on PLM and T is the sampling interval that in the present work is chosen as 1 MW. The FFT method to obtain PLM is depicted in Figure 6. The FFT process reduces the computation time drastically and is highly efficient compared to the conventional method to obtain PLM.

$$N = 2^S, \tag{14}$$

$$f(x) = \sum_{m=1}^{r} a_m \delta(x - b_m), \tag{15}$$

$$g(x) = \sum_{k=0}^{N-1} a_k \delta(x - k \cdot \Delta x), \tag{16}$$

$$F(n) = \sum_{k=0}^{N-1} a_k W^{-nk}, \tag{17}$$

$$\left.\begin{aligned} y_k &= \sum_{n=0}^{N-1} F(n) W^{nk} \\ f(n) &= \sum_{k=0}^{N-1} y_k \delta(x - k \cdot \Delta x) \end{aligned}\right\}, \tag{18}$$

$$N \geq \frac{T_0}{T}. \tag{19}$$

4.2. Reliability Indices Calculation Using PLM. The PLM obtained using the FFT algorithm involves a convolution process multiple times, which also results in continuous modification of PLM, thereby changing the equivalent peak load in the representation. If the number of generating units in the system is "m," having overall capacity U_t, the PLM, after all the generating units have convolved, is represented by the curve $f^{(m)}(x)$. The peak load of the system is modified to a value of $(x_m + U_t)$, illustrated in Figure 7. The conclusive modified PLM is used to obtain the loss of load probability (LOLP) and expected energy not served (EENS),

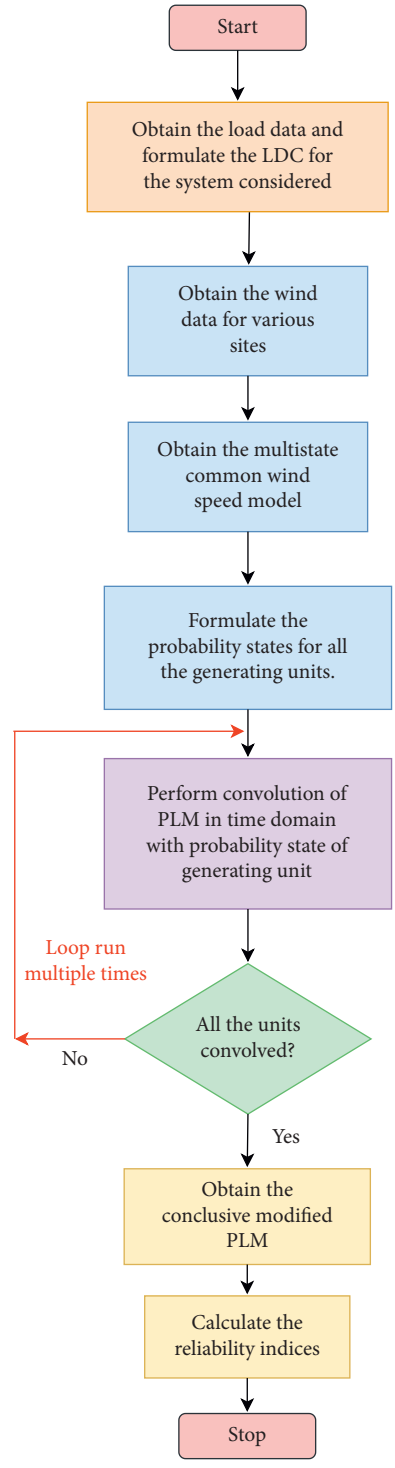

Figure 8: Conventional methodology for reliability evaluation.

which are the indices obtained for the assessment of the reliability of the system. The present work considers generation reliability assessment taking into account generation adequacy, which is accurately represented by LOLP and EENS [34, 35]. LOLP is the probability that the maximum daily load of the system is greater than the capacity of generation and is given by (20), where S is the set of states

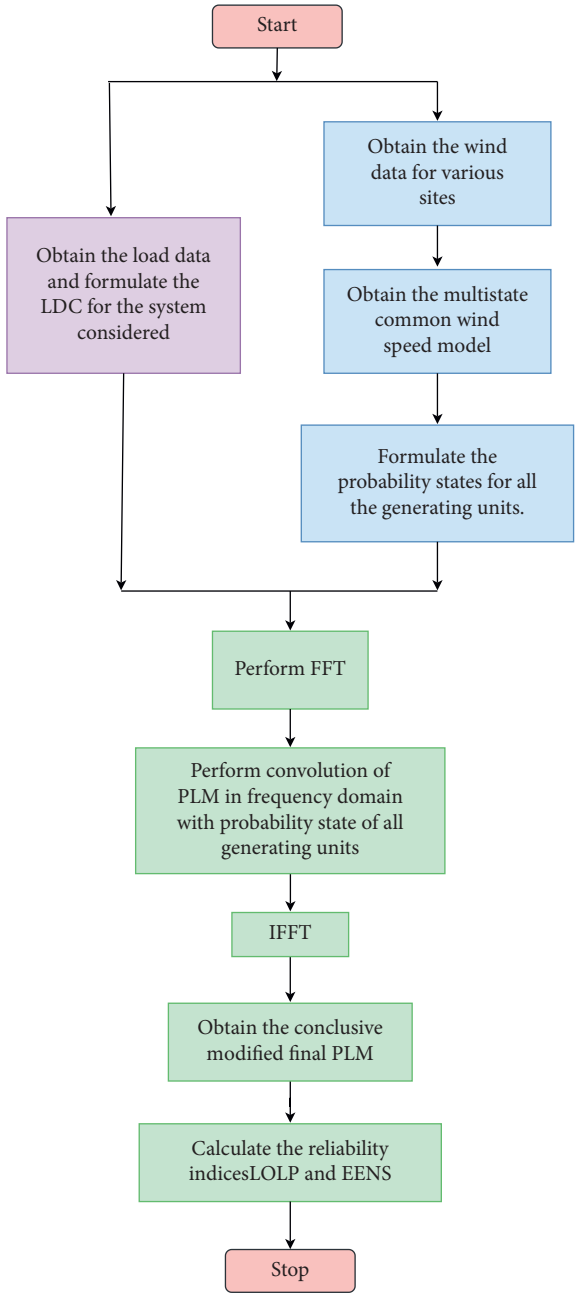

Figure 9: Proposed FFT methodology for reliability evaluation.

that are associated with the loss of load, p_i is the probability of the system state "i," and t_i is the duration related to loss of load for system state "i." EENS is the total energy not served when the load of the system is greater than the generation capacity and is given by (21) [35, 36], where U_i is the generation capacity at state "i" and $(x_m - U_i)$ is the load curtailment. The LOLP and EENS can be obtained from PLM as given by (22) and (23). LOLP from PLM can be obtained in terms of the probability of loss of load for a given time duration, as shown in Figure 7. The PLM combines the probability of loss of load for given states and capacity of loss, as shown in Figure 7. It can be observed from Figure 7 and (22) and (23) that when the load is increased with generation fixed, the indices also increase with the increase in outage capacity.

Table 1: Generator forced outage rate data.

Capacity of unit (MW)	Type	Forced outage rate (FOR)
400×2	Nuclear	0.12
350×1	Coal/steam	0.08
197×3	Oil/steam	0.05
155×4	Coal/steam	0.04
100×3	Oil/steam	0.04
76×4	Coal/steam	0.02
50×6	Hydro	0.01
20×4	Oil/CT	0.10
12×5	Oil/steam	0.02

Table 2: Ten-step wind speed model for San Frisco Bay Area.

Midpoint of wind speed state	Probability
−3.6182	0
−1.0325	0
1.5532	0.0344
4.1389	0.3154
6.7246	0.3567
9.3103	0.2204
11.8960	0.0482
14.4817	0.0207
17.0674	0.0028
19.6531	0

Table 3: Ten-step wind speed model for Contra Costa County.

Midpoint of wind speed state (m)	Probability
−7.1722	0
−3.6231	0
−0.0741	0.0096
3.4750	0.3817
7.0241	0.3010
10.5732	0.2408
14.1222	0.0547
17.6713	0.0096
21.2204	0.0027
24.7695	0

Table 4: Common wind speed model.

Output power of wind farm (MW)	Probability
0	0.3706
97.866	0.3286
437.0464	0.2306
1,028.524	0.0516
1,526	0.0180

$$\text{LOLP} = \sum_{i \in S} p_i t_i, \tag{20}$$

$$\text{EENS} = \sum_{i \in S} 8760 * (x_m - U_i) * p_i, \tag{21}$$

$$\text{LOLP} = f^{(m)}(U_t), \tag{22}$$

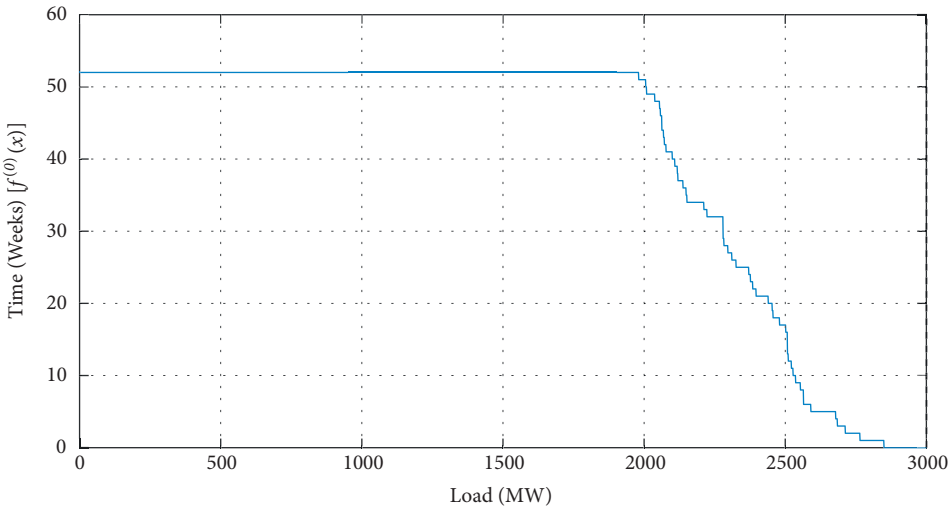

Figure 10: Original load duration curve for RTS-wind [3].

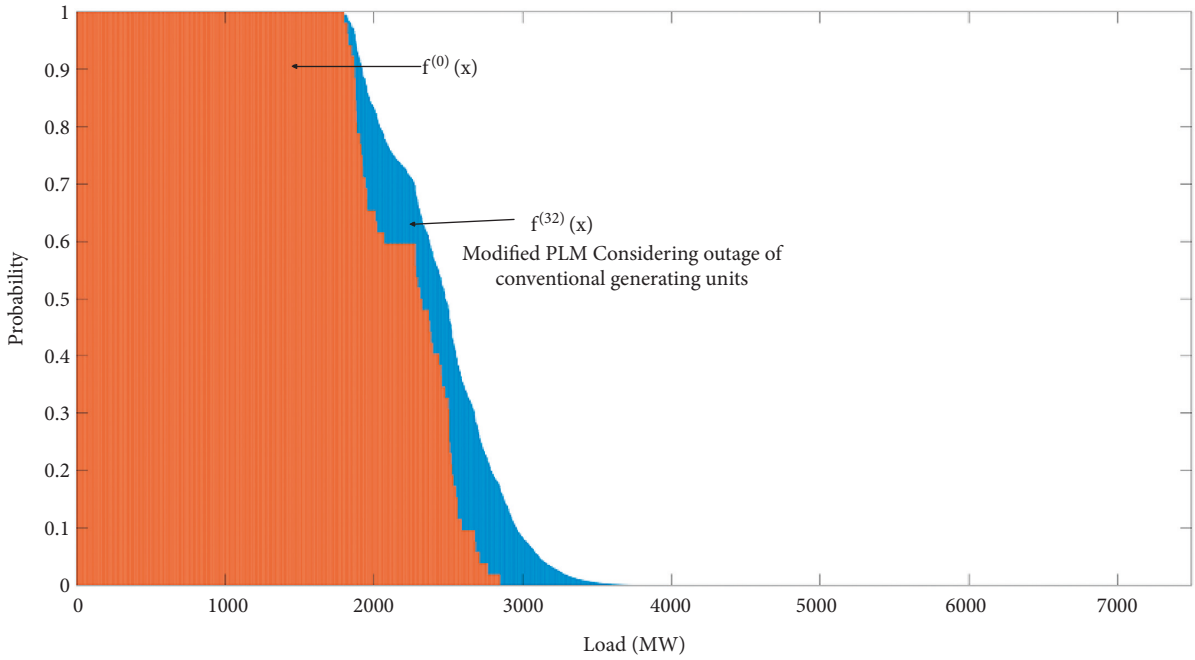

Figure 11: Modified PLM considering outage of DUs.

$$\text{EENS} = \sum_{U_t}^{x_m+U_t} f^m(x). \tag{23}$$

4.3. Reliability Evaluation Methodology. The reliability evaluation involves obtaining load data for the system considered to formulate the PLM. Wind data for different sites is obtained, and each wind site represents a single wind farm. To avoid the representation of different wind farms with different characteristics, a wind speed model that can represent all the wind sites having common characteristics has been used in the present work. FFT is performed on the initial PLM and probability states of generating units. All the generating units are convolved with the PLM in a single step to obtain the final PLM representing the generator outages and wind uncertainty. The reliability indices for reliability assessment are finally obtained. The proposed methodology eliminated the loop, which is run multiple times to convolve the initial PLM with all the generating units. The conventional methodology is shown in Figure 8, and the proposed methodology is shown in Figure 9.

5. Results and Discussion

The proposed methodology is validated by application to IEEE RTS-wind [3]. The IEEE RTS system has been used to validate and benchmark various reliability algorithms. The

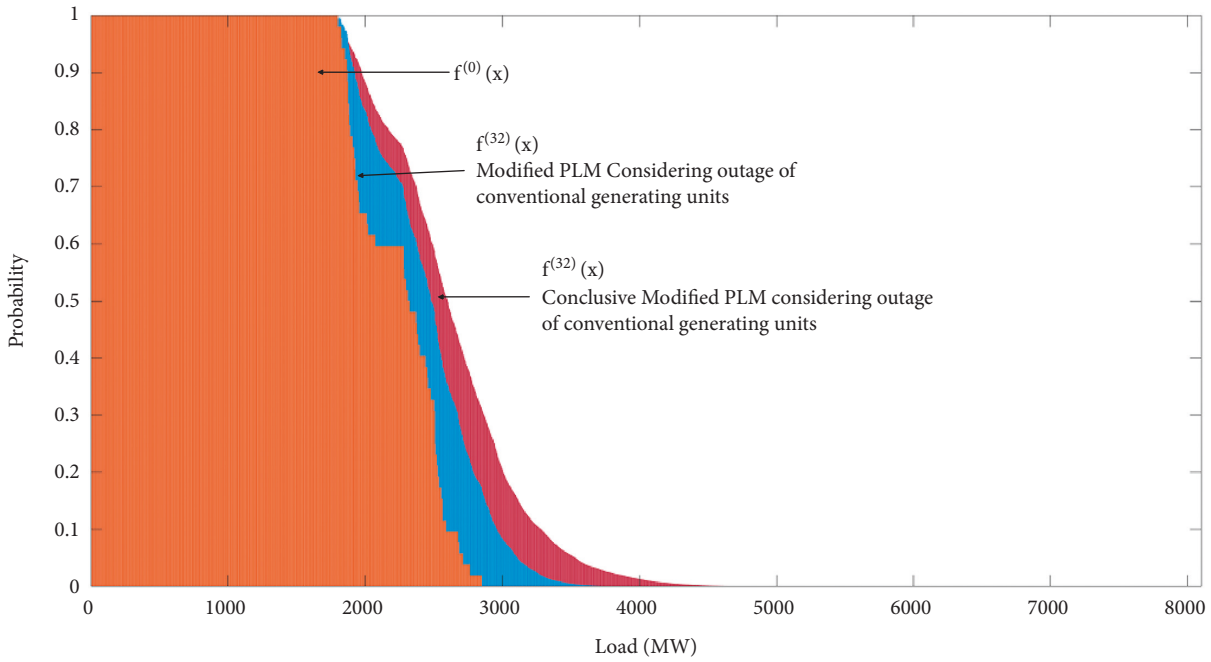

Figure 12: Conclusive modified PLM considering outage of DUs and wind power variability.

Table 5: Reliability index values for wind variability and outage of different percentage of generating units.

Outage percentage of conventional units with respect to effective generation for IEEE RTS-Wind	LOLP	EENS
30.2790% (outage of oil units)	0.000044	0.0205
40.9538% (outage of oil + hydro units)	0.000046	0.0223
66.2261% (outage of oil + hydro + coal units)	0.000102	0.0678
100% (outage of all units)	0.0092	11.2956

conventional IEEE RTS comprises 32 DUs, with a total generation capacity of 3,405 MW, and the maximum connected load in the system is 2,850 MW. The conventional system is modified to RTS-wind by replacing a 350 MW generating unit with a wind farm, consisting of 763 wind turbines with a rated capacity of 2 MW. The forced outage rate (FOR) of conventional generators is listed in Table 1, along with their rated capacity.

The present work considers wind data from two sites in California, USA, where each site is considered a wind farm. The wind data is obtained for a duration of two years, and the locations chosen are San Francisco Bay Area and Contra Costa County from [32]. The mean speed and standard deviation of the San Francisco Bay Area are 6.7246 and 2.5857, respectively; also, the mean and standard deviation of the Contra Costa County are 7.0241 and 3.5491, respectively. The 10-step speed models for the 2 sites are shown in Tables 2 and 3, respectively. Combining the probabilities of the two sites, the common wind speed model is shown in Table 4; two wind farms are represented by a common power and probability model. The present work considers Enercon E82 wind turbine [37], with cut-in speed of 4 (m/s), cut-out speed of 28 (m/s), rated speed 15 (m/s), and the rated power 2 (MW).

The LDC for the considered IEEE RTS-wind system is shown in Figure 10, representing the variation of load with time in weeks. The LDC has a maximum load of 2,850 MW, which all the generating units cater to during normal operation. The PLM is obtained from the convolution of LDC, and probabilistic outages of all the connected DUs are shown in Figure 11. The PLM has a maximum load of 6,255 MW, considering the outage of all the generating units. The conclusive modified PLM plot considering the variability of power of wind farms is shown in Figure 12; the maximum load of the PLM shifts to 7,431 MW. The LOLP and EENS have been obtained from the curves.

The reliability indices for the outage of different percentage of generation with wind variation are presented in Table 5. It can be observed with the outage of a lesser percentage of generating units that the reliability of the system is very high and decreases with an increase in the outage of the generating units. The reliability indices calculated from FFT-based PLM for different cases representing different load percentages are shown in Table 6. It can be observed that the reliability has increased with the inclusion of wind farms, as a large capacity wind farm (763×2 MW) is included in place of a 350 MW generator. It can also be observed that as the load increases, the reliability of the system decreases. When the system is underloaded, the reliability of the system is high; as the load of the system increases by 10%, the system is reliable as compared to the conventional system. However, when the load increases by 20%, the reliability of the system slightly decreases. The reliability indices using the time-domain approach are also

Table 6: Reliability index calculation using various approaches.

Type of system	Frequency-domain approach		Time-domain approach	
	Loss of load probability (LOLP)	Expected energy not served (EENS) in GWh/yr	Loss of load probability (LOLP)	Expected energy not served (EENS) in GWh/yr
IEEE RTS	0.009157	11.2960	0.0092	11.2956
IEEE RTS-wind	0.001077	1.4300	0.001077	1.4290
IEEE RTS-wind (80% load)	0.000023	0.0003	0.000023	0.0003
IEEE RTS-wind (90% load)	0.000197	0.0040	0.000196	0.0040
IEEE RTS-wind (110% load)	0.003686	6.3030	0.003683	6.2951
IEEE RTS-wind (120% load)	0.009788	20.7651	0.009789	20.7648

presented in Table 6; the indices are almost similar as compared to the reliability indices obtained using frequency-domain approach, which proves the precision of the proposed frequency-domain approach.

6. Conclusion

The replacement of conventional energy sources with renewable energy resources demands efficient and simplistic algorithms for generation planning. PLM serves as an important tool in generation planning to determine the reliability of the system. However, integrating a multistate wind model is challenging and requires the simulation process to run multiple times. The present work has extended the conventional two-state generation model considering generator outages to include multistate NDUs in generation planning. Also, the complexity of computation associated with multistate models is alleviated by using the frequency-domain approach using FFT. The efficacy of the proposed approach has been validated through case studies using a standard test system such as IEEE RTS and IEEE RTS-wind. Since the NDUs have a lower capacity factor compared to DUs, therefore, more NDU capacity addition is required to maintain the same reliability indices compared to the DUs. The reliability indices such as LOLP and EENS of IEEE RTS-wind are comparable with those of the original IEEE RTS system when about four times wind energy generation is integrated into the system. Thus, proper generation planning can ensure reliability even when NDUs are integrated into the power system.

Data Availability

All data used to support the findings of the study are included within the article.

Conflicts of Interest

The authors declare that there are no conflicts of interest.

References

[1] A. T. D. Perera, V. M. Nik, D. Mauree, and J.-L. Scartezzini, "Electrical hubs: an effective way to integrate non-dispatchable renewable energy sources with minimum impact to the grid," *Applied Energy*, vol. 190, pp. 232–248, 2017.

[2] D. Kumar, D. K. Mohanta, and M. J. B. Reddy, "Intelligent optimization of renewable resource mixes incorporating the effect of fuel risk, fuel cost and CO_2 emission," *Frontiers in Energy*, vol. 9, no. 1, pp. 91–105, 2015.

[3] A. M. Leite da Silva, J. F. D. Costa Castro, and R. Billinton, "Probabilistic assessment of spinning reserve via cross-entropy method considering renewable sources and transmission restrictions," *IEEE Transactions on Power Systems*, vol. 33, no. 4, pp. 4574–4582, 2018.

[4] C. Jung and D. Schindler, "The role of the power law exponent in wind energy assessment: a global analysis," *International Journal of Energy Research*, vol. 45, no. 6, pp. 8484–8496, 2021.

[5] S. G. Kadwane and D. K. Mohanta, "Reliability evaluation of overall wind energy conversion system incorporating power electronic inverter," *International Journal of Reliability and Safety*, vol. 7, no. 4, p. 319, 2013.

[6] M. Manohar, E. Koley, S. Ghosh, D. K. Mohanta, and R. C. Bansal, "Spatio-temporal information based protection scheme for PV integrated microgrid under solar irradiance intermittency using deep convolutional neural network," *International Journal of Electrical Power & Energy Systems*, vol. 116, Article ID 105576, 2020.

[7] S. Kumar, R. K. Saket, D. K. Dheer, J. B. Holm-Nielsen, and P. Sanjeevikumar, "Reliability enhancement of electrical power system including impacts of renewable energy sources: a comprehensive review," *IET Generation, Transmission & Distribution*, vol. 14, no. 10, pp. 1799–1815, 2020.

[8] S. F. Santos, D. Z. Fitiwi, A. W. Bizuayehu et al., "Impacts of operational variability and uncertainty on distributed generation investment planning: a comprehensive sensitivity analysis," *IEEE Transactions on Sustainable Energy*, vol. 8, no. 2, pp. 855–869, 2017.

[9] J. Vardi, J. Zahavi, and B. Avi-Itzhak, "The combined load duration curve and its derivation," *IEEE Transactions on Power Apparatus and Systems*, vol. 96, no. 3, pp. 978–983, 1977.

[10] L. Ge, W. Liao, S. Wang, B. Bak-Jensen, and J. R. Pillai, "Modeling daily load profiles of distribution network for scenario generation using flow-based generative network," *IEEE Access*, vol. 8, pp. 77587–77597, 2020.

[11] J. G. Proakis and D. G. Manolakis, *Digital Signal Processing*, Pearson, London, UK, 5th edition, 2021.

[12] N. Liu and P. Crossley, "Assessing the risk of implementing system integrity protection schemes in a power system with significant wind integration," *IEEE Transactions on Power Delivery*, vol. 33, no. 2, pp. 810–820, 2018.

[13] X. Liu, J. Ospina, and C. Konstantinou, "Deep reinforcement learning for cybersecurity assessment of wind integrated power systems," *IEEE Access*, vol. 8, pp. 208378–208394, 2020.

[14] Y. Li, Z. Ni, T. Zhao et al., "Coordinated scheduling for improving uncertain wind power adsorption in electric vehicles—wind integrated power systems by multiobjective

optimization approach," *IEEE Transactions on Industry Applications*, vol. 56, no. 3, pp. 2238–2250, 2020.

[15] M. Sharma, S. Dhundhara, Y. Arya, and S. Prakash, "Frequency excursion mitigation strategy using a novel COA optimised fuzzy controller in wind integrated power systems," *IET Renewable Power Generation*, vol. 14, no. 19, pp. 4071–4085, 2020.

[16] S. R. Das, P. K. Ray, A. K. Sahoo et al., "Performance of hybrid filter in a microgrid integrated power system network using wavelet techniques," *Applied Sciences*, vol. 10, no. 19, p. 6792, 2020.

[17] T. Ding, S. Liu, W. Yuan, Z. Bie, and B. Zeng, "A two-stage robust reactive power optimization considering uncertain wind power integration in active distribution networks," *IEEE Transactions on Sustainable Energy*, vol. 7, no. 1, pp. 301–311, 2016.

[18] R. Billinton, R. Karki, Y. Gao, D. Huang, P. Hu, and W. Wangdee, "Adequacy assessment considerations in wind integrated power systems," *IEEE Transactions on Power Systems*, vol. 27, no. 4, pp. 2297–2305, 2012.

[19] T. K. Shrestha and R. Karki, "Utilizing energy storage for operational adequacy of wind-integrated bulk power systems," *Applied Sciences*, vol. 10, no. 17, p. 5964, 2020.

[20] R. Karki, P. Hu, and R. Billinton, "A simplified wind power generation model for reliability evaluation," *IEEE Transactions on Energy Conversion*, vol. 21, no. 2, pp. 533–540, 2006.

[21] S. Sulaeman, M. Benidris, J. Mitra, and C. Singh, "A wind farm reliability model considering both wind variability and turbine forced outages," *IEEE Transactions on Sustainable Energy*, vol. 8, no. 2, pp. 629–637, 2017.

[22] H. Kim, C. Singh, and A. Sprintson, "Simulation and estimation of reliability in a wind farm considering the wake effect," *IEEE Transactions on Sustainable Energy*, vol. 3, no. 2, pp. 274–282, 2012.

[23] N. Nguyen and J. Mitra, "Reliability of power system with high wind penetration under frequency stability constraint," *IEEE Transactions on Power Systems*, vol. 33, no. 1, pp. 985–994, 2018.

[24] S. Thapa, R. Karki, and R. Billinton, "Utilization of the area risk concept for operational reliability evaluation of a wind-integrated power system," *IEEE Transactions on Power Systems*, vol. 28, no. 4, pp. 4771–4779, 2013.

[25] X. Yang, Y. Yang, Y. Liu, and Z. Deng, "A reliability assessment approach for electric power systems considering wind power uncertainty," *IEEE Access*, vol. 8, pp. 12467–12478, 2020.

[26] A. M. Khalkho, B. Rapada, G. Majumder, M. Cherukuri, and D. K. Mohanta, "Impact assessment of solar power generation uncertainty on smart grid reliability and carbon neutrality," *Frontiers in Energy Research*, vol. 10, 2022.

[27] A. Abiri-Jahromi, M. Fotuhi-Firuzabad, and M. Parvania, "Optimized midterm preventive maintenance outage scheduling of thermal generating units," *IEEE Transactions on Power Systems*, vol. 27, no. 3, pp. 1354–1365, 2012.

[28] D. K. Mohanta, P. K. Sadhu, and R. Chakrabarti, "Fuzzy reliability evaluation of captive power plant maintenance scheduling incorporating uncertain forced outage rate and load representation," *Electric Power Systems Research*, vol. 72, no. 1, pp. 73–84, 2004.

[29] X. Wang and J. Mcdonald, *Modern Power System Planning*, McGraw-Hill Education, New York, NY, USA, 1993.

[30] J. A. Carta and D. Mentado, "A continuous bivariate model for wind power density and wind turbine energy output estimations," *Energy Conversion and Management*, vol. 48, no. 2, pp. 420–432, 2007.

[31] H. Liu, J. Shi, and X. Qu, "Empirical investigation on using wind speed volatility to estimate the operation probability and power output of wind turbines," *Energy Conversion and Management*, vol. 67, pp. 8–17, 2013.

[32] Datasets and Climate Data Online (CDO), "National climatic data center (NCDC)," 2021, https://www.ncdc.noaa.gov/cdo-web/datasets#GHCND.

[33] S. R. Lakshmi, S. C. Tripathy, K. S. P. Rao, and R. Balasubramianian, "Evaluation of generation system reliability indices by fast transform techniques," *International Journal of Electrical Power & Energy Systems*, vol. 17, no. 4, pp. 281–287, 1995.

[34] A. Ghaedi, A. Abbaspour, M. Fotuhi-Firuzabad, and M. Moeini-Aghtaie, "Toward a comprehensive model of large-scale DFIG-based wind farms in adequacy assessment of power systems," *IEEE Transactions on Sustainable Energy*, vol. 5, no. 1, pp. 55–63, 2014.

[35] T. Adefarati, R. C. Bansal, and J. J. Justo, "Reliability and economic evaluation of a microgrid power system," *Energy Procedia*, vol. 142, pp. 43–48, 2017.

[36] R. Billinton and W. Li, *Reliability Assessment of Electric Power Systems Using Monte Carlo Methods*, Springer, Berlin, Germany, 1994.

[37] M. Singh and S. Santoso, *Dynamic Models for Wind Turbines and Wind Power Plants*, National Renewable Energy Lab, Golden, CO, USA, 2011.